PROCEEDINGS, 42nd Workshop on Geothermal Reservoir Engineering
Stanford University, Stanford, California, February 13-15, 2017
SGP-TR-212

Trial Deployment of a Surface Heat Flow Probe Over the Los Azufres Geothermal Region, Mexico

Graeme Beardsmore[1], Luis Gutiérrez-Negrín[2], Víctor Garduño-Monroy[2], O.M. Espinoza-Ojeda[2], Salvador Almanza-Álvarez[2], Anson Antriasian[1], Shannon Egan[1]

[1] Hot Dry Rocks Pty Ltd, PO Box 251, South Yarra VIC 3141, AUSTRALIA

[2] CeMIE-Geo, Morelia, Michoacán, Mexico

graeme.beardsmore@hotdryrocks.com

Keywords: Heat Needle, Heat flow, Los Azufres, Mexico, Exploration

ABSTRACT

We deployed six 'Heat Needle' probes in and around the Los Azufres geothermal field in Michoacán, Mexico, over a six-month period from September 2014 to March 2015, to assess their functionality for geothermal surveying. The trial was part of Project 23 of the Mexican Center for Geothermal Energy Innovation (CeMIE-Geo): Testing probes for measuring shallow heat flow in geothermal zones.

Los Azufres is the second largest and oldest geothermal field in Mexico, with an installed geothermal electric capacity of 247.8 MW_e. The geothermal field was chosen for this trial because its underlying hydrothermal system is reasonably well understood. Five Heat Needles were distributed across the geothermal field at spacings between one and four kilometers, with a sixth Heat Needle placed in a location of assumed 'background' heat flow outside the geothermal field.

Each Heat Needle precisely recorded thermal gradient in the top 1.10 m of soil at 15-minute intervals for the duration of the trial, and made a single measurement of the thermal conductivity profile of the soil. Combining the thermal gradient records with the thermal conductivity measurements showed the ebb and flow of surface conductive heat flow due to insolation and re-radiation at each site to an absolute precision of about ± 0.02 W/m^2. As expected, the observed heat flow pulsed rhythmically each 24-hour period. After filtering the diurnal signal by taking the average of each interval of 96 consecutive records, the resulting mean daily heat flow records drifted by at least 3 W/m^2 at each site over the six-month survey, mostly due to the seasonal surface temperature cycle. Fluctuations of 1–2 W/m^2 associated with the passage of weather systems were obvious over periods of several weeks. Many of the weather-related fluctuations, however, were strongly correlated between Heat Needle sites, with a detectable mean offset between sites attributed to variations in subsurface heat sources.

Rudimentary data processing defined (within a range of ± 0.5 W/m^2) positive offsets in the subsurface component of heat flow at four of the sites relative to the 'background' site. Heat flow at the fifth site was not significantly higher than background at the achieved level of precision. The heat flow detected by the Heat Needles and attributed to subsurface sources was comparable to estimates of heat flow from deep geothermal wells in the field.

Heat Needles show great potential for delineating shallow thermal features such as outflow pathways or permeable fractures, constraining the total heat flux from a geothermal system, or constraining the lateral extent of deep thermal anomalies with carefully designed surveys.

1. INTRODUCTION

1.1. Background

We deployed six 'Heat Needle' probes (under development by Hot Dry Rocks Pty Ltd, Australia) in and around the Los Azufres geothermal field, approximately 50 km east of Morelia in Michoacán, Mexico (Figure 1), over a six-month period from September 2014 to March 2015. The trial was carried out as part of Project 23 of the Mexican Center for Geothermal Energy Innovation (CeMIE-Geo): Testing probes for measuring shallow heat flow in geothermal zones. The purpose of the trial was to assess the functionality of Heat Needles for detecting and quantifying anomalous surface conductive heat flow. Los Azufres was one of four sites chosen for Project 23 because its underlying geothermal system is reasonably well understood. Results from the three other sites will be reported elsewhere.

1.2. The Los Azufres geothermal field

Los Azufres is the second largest and oldest geothermal field in Mexico, lying at an average altitude of 2,850 meters above sea level in the geographic province of the Trans-Mexican Volcanic Belt. The geothermal field comprises 42 production wells and six reinjection wells scattered throughout a pine forest near private and public resort facilities built around the hydrothermal system's hot springs. The current installed geothermal electrical generating capacity at Los Azufres is 247.8 MW_e, comprising six flash steam condensing units (4 x 26.6 MW_e, 1 x 50 MW_e, 1 x 53.4 MW_e), seven back-pressure units (5 MW_e each) and two binary cycle units (1.5 MW_e each). The running capacity, however, is 224.8 MW_e, since five of the back-pressure units and the two binary cycle units are currently out of operation. A fifth 26.6 MW_e flash steam condensing unit is currently under construction to make more efficient use of the steam. The state-run utility, Comision Federal de Electricidad (CFE), owns and operates all the power units, wells and superficial installations.

Figure 1: (Blue rectangle) Approximate area of the Los Azufres geothermal field to the east of Morelia, Michaocán, Mexico.

The pre-volcanic regional basement is composed of metamorphic and sedimentary rocks of Late Mesozoic to Oligocene age, including gently folded and metamorphosed shales, sandstones, and conglomerates. While these basement rocks are assumed to underlie the geothermal field, not even the deepest well (well AZ-44 at 3544 m) has reached them. The oldest volcanic rocks outcropping in the vicinity are andesites from about 18 Ma, and micro-granular andesites from 5.9 ± 0.6 Ma. These rocks are highly fractured, faulted and exhibit sedimentary-type layering in some parts (Gutiérrez-Negrín and Aumento, 1982). Some geothermal wells have intersected basaltic and diabase dikes intruding the andesitic package.

The andesites are overlain by Quaternary (1.2 ± 0.4 Ma) rhyolites with fluidal and perlite structures and some obsidian flows, which outcrop mainly in the central-south portion of the geothermal field. The rhyolites are hydrothermally altered to kaolin by geothermal fluids discharging at the surface in some places (Dobson and Mahood, 1985; Pérez-Esquivias *et al.*, 2010). Rhyodacites and dacites up to 0.15 Ma in age stratigraphically overlie the Quaternary rhyolites. These silicic rocks tend to form domes and short lava flows with glassy structures. They have been grouped into five distinct lithological units with a combined thickness of about 1,000 m, namely Agua Fría Rhyolite, Tejamaniles Dacite, Cerro Mozo Dacite, San Andrés Dacite and Yerbabuena Rhyolite. In general, these rocks are highly fractured (Pérez Esquivias *et al.*, 2010). The youngest outcropping rocks include porphyritic andesites, glassy and pumicitic rhyolites, and basalt flows and cinder cones on the western part of the geothermal field (Dobson and Mahood, 1985).

Most of the rocks in the field have been affected to some extent by hydrothermal fluids. Hydrothermal effects include vesicle and fracture fillings and alteration of primary minerals. The hydrothermal activity can be divided into two types: acid sulfate near the surface, and alkali chloride below the water table, which lies at about 400 m depth (Viggiano-Guerra and Gutiérrez-Negrín, 1995).

The region is in a compressional tectonic regime related to subduction, but with local extension. The main structures in the Los Azufres geothermal field trend NNW–SSE, NE–SW and E–W (Figure 2). The first fracture system was produced during a Miocene deformation event, with sub-vertical geometry affecting the basement. The two other systems affect the Miocene basement and Quaternary rocks outcropping in the geothermal field (Pérez Esquivias *et al*., 2010), and have sub-vertical and sub-horizontal geometry.

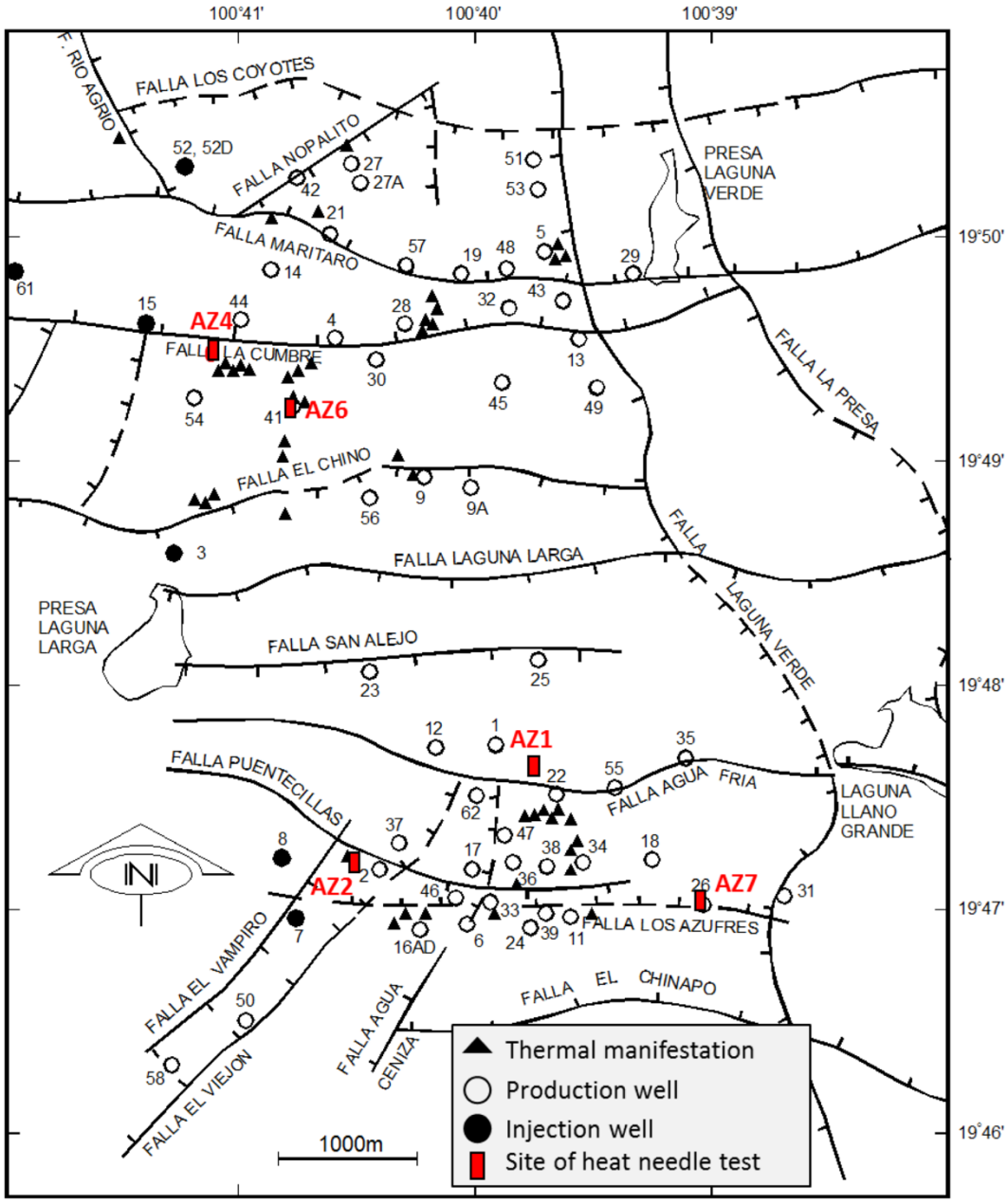

Figure 2: Wells locations, identified structures, thermal manifestations and Heat Needle deployment sites across the Los Azufres geothermal field. Figure modified after Arellano *et al.* (2015).

The geological setting represents a CV-1a geothermal play type (as defined by Harvey *et al.*, 2016), a convection dominated geothermal system related to an active or recent magmatic intrusion. Surface geothermal manifestations include hot springs with temperatures up to 90°C, fumaroles, steaming soils, mud pools and small thermal lakes. There is a strong correlation between the locations of surface manifestations and the surface expression of faults and lineaments (Figure 2), suggesting that fluid movement is dominantly controlled by fractures (Viggiano-Guerra and Gutiérrez-Negrín, 1995).

The geothermal reservoir is hosted within a series of more than 2,700 m thick interstratified lava flows and pyroclastic rocks of andesitic to basaltic composition, with minor rhyolites. It is overlain at depth by rocks from the five rhyolitic units described above. The main geothermal reservoir is steam dominated (currently ~73% steam) and the heat source is the magma chamber of the San Andrés Volcano (Gutiérrez-Negrín, 2015). The geothermal fluids of the reservoir are of sodium chloride type with high CO_2 content, and pH ~7.5. The reservoir is typically at 240°C to 280ºC, but the highest recorded temperature is ~320ºC. The main non-condensable gases (NCG) in the separated steam are CO_2 (94% of NCG by volume), H_2S (2.5%) and minor concentrations of H_2, CH_4, N_2 and NH_3 (combined 3.5%) (Barragán-Reyes *et al.*, 2012).

1.3. Heat Needles

Heat Needles are self-contained instruments for measuring conductive heat flow in the top meter of the Earth. They combine a series of accurate and sensitive thermometers with onboard memory and a heating element for 'line source' thermal conductivity measurements. Beardsmore (2012) and Beardsmore and Antriasian (2015) provided details on the design, early development and calibration of Heat Needles. The six Heat Needles used in this trial were third generation devices deployed in a vertical orientation (± 2°). A 16 mm diameter stainless steel casing was first inserted in the ground using a hand-operated electric hammer drill (Figure 3). The sensors were subsequently inserted to record temperature to ± 0.0003°C precision and ± 0.003°C absolute accuracy at 15-minute intervals at ground surface level, and at 0.10 m, 0.30 m, 0.50 m, 0.70 m, 0.90 m and 1.10 m depth. The average of 96 consecutive records gave a 24-hour mean temperature at each depth, effectively filtering the large diurnal fluctuations in near-surface temperature.

Figure 3: Deploying a Heat Needle. (Left) A stainless steel casing was first embedded into the ground. (Middle) A logging unit and string of sensors was inserted into the casing. (Right) The weatherproof, sun-shielded instrument passively recorded ground temperature at regular intervals until it was retrieved.

An *in situ* thermal conductivity measurement of the ground was completed at each site at the end of the six-month trial. Each thermal conductivity measurement involved recording the temperature response of the Heat Needle over a period of one hour, during which it was internally heated at a constant rate of 14.9 W/m along its length. The Heat Needle length-to-diameter ratio exceeded 30:1 for the four sensors from 0.30 m to 0.90 m depth, and so sufficiently approximated an infinite 'full space line source probe' at those depths (Blackwell, 1954). It did not fully meet this criterion at 0.10 m depth, but an approximate conductivity measurement was still possible. Popov *et al.* (2016) quoted Equation 1 for calculating thermal conductivity from a full space line source probe:

$$\lambda = \frac{q'}{4\pi} \cdot \frac{ln\left(\frac{t_2}{t_1}\right)}{T(t_2) - T(t_1)} \quad (1)$$

where λ is the thermal conductivity (W/mK) of the material surrounding the Heat Needle at the depth of a given sensor; q' is the applied heating power (14.9 W/m); and t_1 and t_2 are the times after heating commenced (seconds) at which the Heat Needle sensor recorded temperatures $T(t_1)$ and $T(t_2)$ (°C), respectively. In practice, a measurement involved calculating the gradient of a plot of temperature versus the natural log of time after heating commenced once the curve reached linearity.

Vertical conductive heat flow at any given time (Q_t, W/m^2) is the product of the thermal gradient at that time (δT_t / δz, K/m) and the thermal conductivity (λ, W/mK):

$$Q_t = \lambda \, . \, \delta T_t / \delta z \quad (2)$$

Where thermal conductivity varies with depth, heat flow can alternatively be calculated as the gradient of temperature versus thermal resistance (R, m^{2}K/W):

$$Q_t = \delta T_t / \delta R \quad (3)$$

Where *R* is the physical depth (z) divided by the average thermal conductivity between the surface and depth, z.

Heat Needle data gave a daily average temperature profile, as well as a thermal conductivity profile, at each deployment site. Applying these data to Equation 3 yielded a daily average conductive heat flow at each site. Most of the temporal variation in heat flow recorded over an extended period at each site was due to changes in mean surface temperature over periods longer than 24 hours, in response to weather systems and seasonal cycles. As these longer period signals were similar over broad areas, observed offsets in heat flow *between* sites could be attributed to subsurface causes, especially if the offsets were approximately constant with time. This is the basic premise underpinning the use of Heat Needles for geothermal surveying.

2. SURVEY SITES AND RESULTS

We deployed six Heat Needles for a six-month period from September 2014 to March 2015 around the Los Azufres geothermal field (Figure 4). Five Heat Needles (sites AZ1, AZ2, AZ4, AZ6 and AZ7) were distributed across the geothermal field at spacings between one and four kilometers, with a sixth Heat Needle (site AZ8) placed in a location of assumed 'background' heat flow outside the geothermal field. We selected the sites based on accessibility, security and proximity to known or suspected geothermal features. The field trial was not intended as an exploration or mapping exercise, but rather a test of the functionality of Heat Needles under field conditions. Other researchers have previously demonstrated that a maximum spacing of two to three hundred meters is required to image ground temperature and heat flow variation around active geothermal systems (eg Coolbaugh *et al.*, 2014).

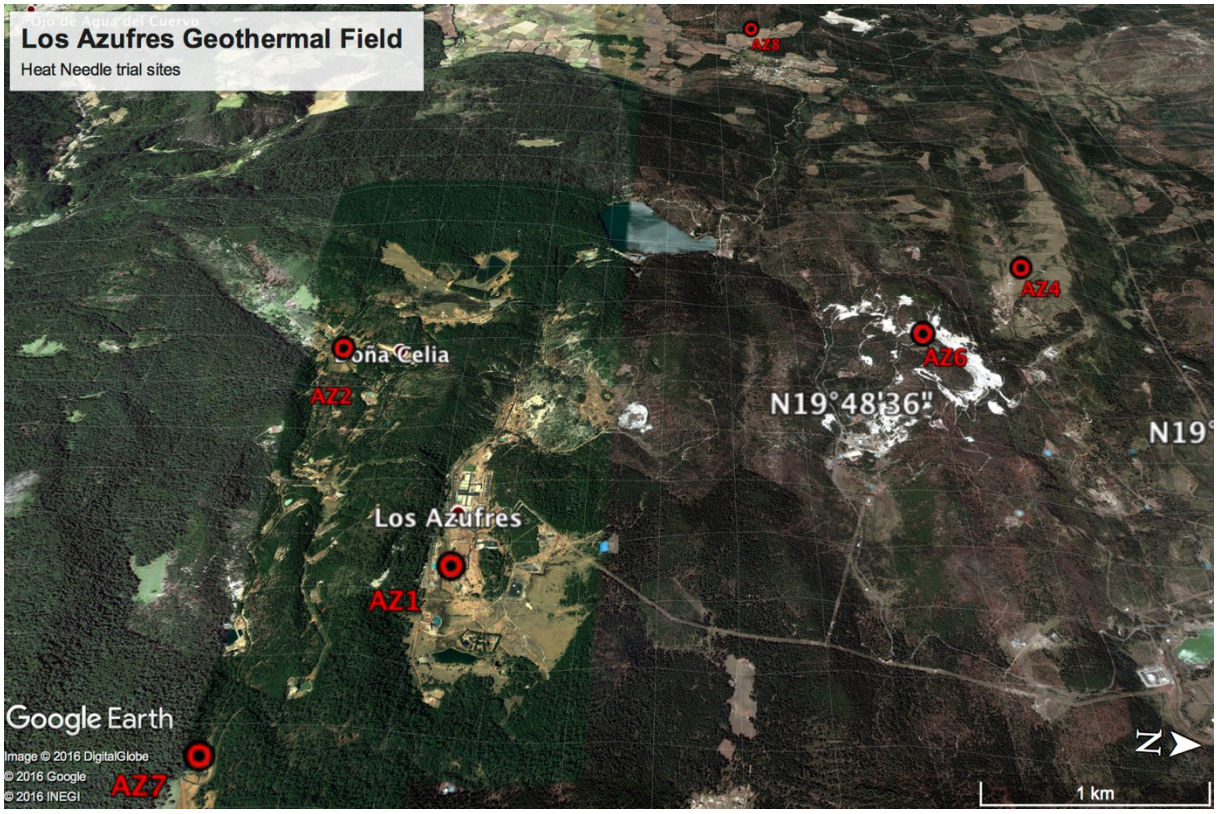

Figure 4: Google Earth view of Heat Needle survey sites, looking west over the Los Azufres geothermal field. Grid size is 400 m.

Our goal was to collect two sets of data at each site:

- Temperature at the air–soil interface and at 0.10 m, 0.30 m, 0.50 m, 0.70 m, 0.90 m and 1.10 m depth at 15-minute intervals for the duration of the trial. These data provided precise records of changes in shallow thermal gradient over time.
- The temperature response of the Heat Needle to an active injection of heat over a one-hour period. These data provided information about the thermal conductivity structure of the ground. Conductive heat flow is the product of thermal gradient and thermal conductivity.

2.1 Site AZ1—Residencia de Agua Fría

19.79055 °N, 100.66055 °W UTM coordinates: 14Q, 326050 mE, 2189157 mN Elevation: 2,884 ± 7 m

We deployed one Heat Needle on a grassy expanse inside the grounds of the CFE administrative buildings within the Los Azufres geothermal field (Figure 5). The site was readily accessible and considered secure from public interference.

Figure 5: Google Earth overview of site AZ1, and deploying the Heat Needle on-the-ground.

2.1.1 AZ1 temperature records

The Heat Needle successfully collected a full temperature record for the 181-day period of deployment; approximately 120,000 individual high-precision temperature measurements. Figure 6 shows the full record for the first 30 days of the trial, and Figure 7 the daily mean recorded temperatures (centered on midnight UTC time each day) for the full trial period. The full record confirmed that surface temperature fluctuated on a daily cycle with a peak-to-trough amplitude on the order of 10°C. The 24-hour average effectively filtered the daily volatility and revealed longer period (weeks) fluctuations in mean surface temperature with peak-to-trough amplitudes on the order of 2°C. These were likely related to the passing of weather systems over the trial area. The annual temperature cycle was also evident in the trend of decreasing then increasing surface temperature over the course of the six-month trial.

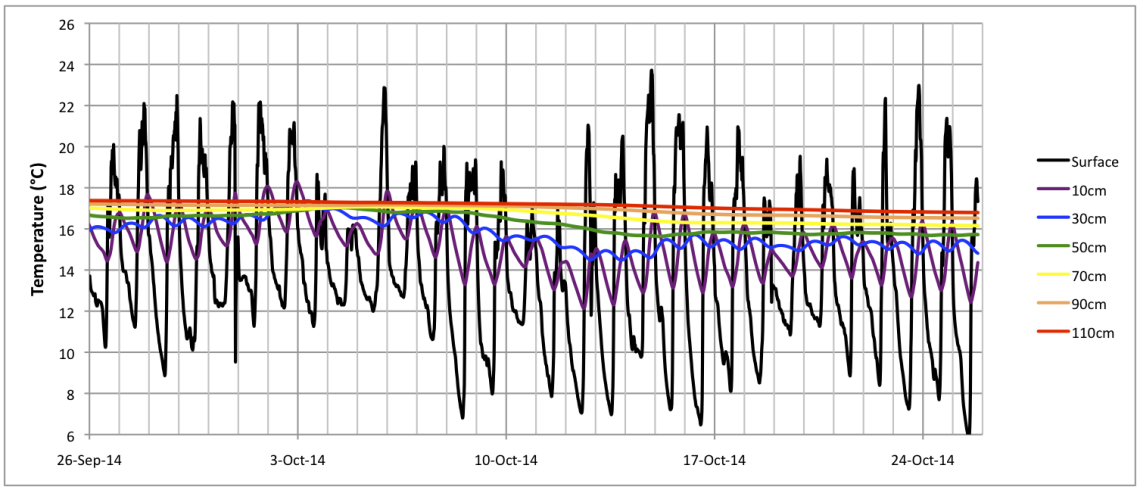

Figure 6: Full temperature record for the first 30 days of the trial at site AZ1. Horizontal grid interval is one day.

Both the full and filtered temperature records captured the diffusion of surface temperature fluctuations into the ground, overprinting a general increase in temperature with depth. As predicted by the 'heat equation' (e.g. Section 2.6 of Carslaw and Jaeger, 1959), progressively deeper sensors recorded an increasing time lag and decay in amplitude of the surface temperature signal, both of which are a function of the thermal inertia of the ground.

2.1.2 AZ1 thermal conductivity and thermal resistance

We carried out a successful one-hour thermal conductivity measurement on 24 March 2015, although some measurement data failed to record due to an intermittent logger error. Figure 8 presents the recorded increase in temperature versus the natural logarithm of heating time for the six sub-surface sensors. We derived the mean thermal conductivity of the ground surrounding each sensor from the gradients of the linear portions of the semi-log plots using the relationship in Equation 1.

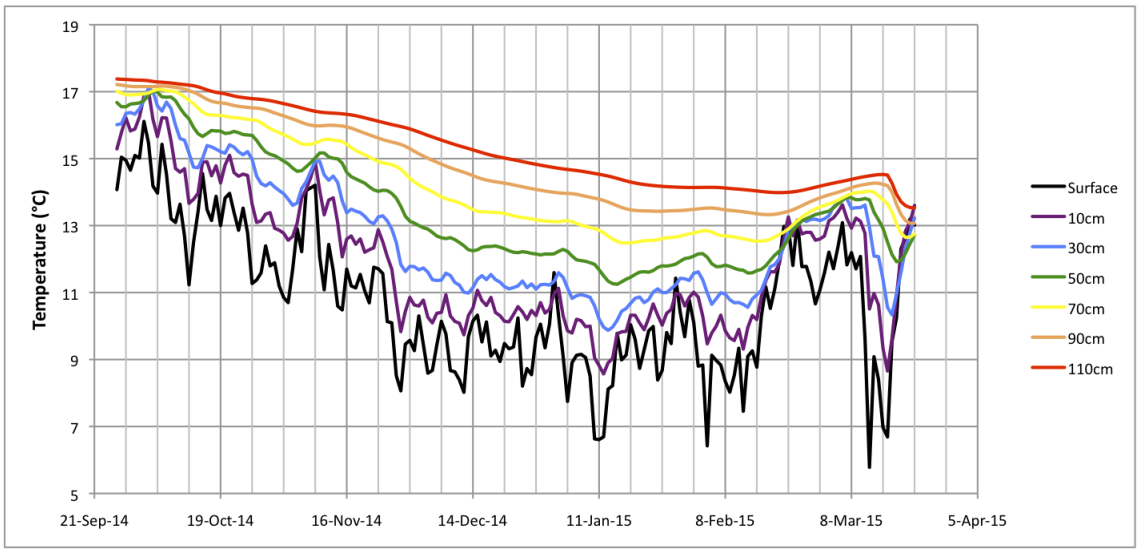

Figure 7: 24-hour mean temperature at each sensor depth, centered on midnight UTC time over the full trial period. Horizontal grid interval is one week.

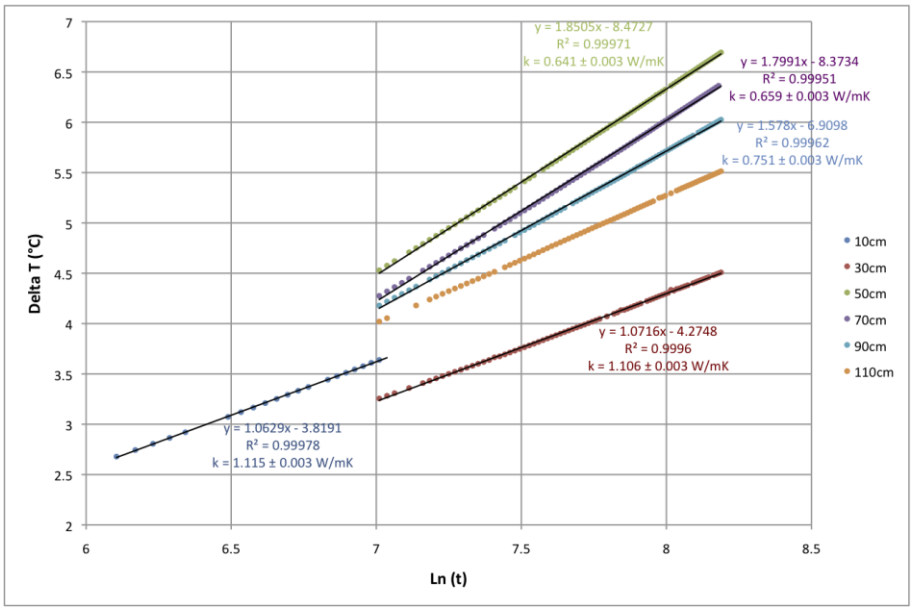

Figure 8: Temperature increase versus natural log of heating time during the thermal conductivity test. Annotations include the equations of the best-fit linear regression lines, and the inferred thermal conductivities (denoted by "k").

The background drift in temperature at 0.10 m depth over the one hour period was great enough to impact on the conductivity calculation, so we inferred the thermal conductivity at 0.10 m over a shorter and early time interval compared to the deeper sensors (Figure 8). The accuracy of the measurement at 0.10 m is thus relatively lower than the other depths. As expected, the sensor at 1.10 m did not yield a reliable conductivity estimate by the same method as the other sensors because its position in the Heat Needle did not meet the requirement for a 'infinite line source' approximation. We later inferred the mean conductivity at 1.10 m by extrapolating the Bullard plot curves presented below.

We calculated the mean conductive surface heat flow each day from the gradient of the best-fit linear regression line through the daily average temperatures versus thermal resistance, following Equation 3. We calculated the thermal resistance between the surface and each sensor depth as the cumulative sum of the physical depth divided by the interval thermal conductivity, assuming each conductivity represented an interval of 0.2 m centered on the sensor depth. Table 1 presents the calculated thermal conductivities and thermal resistances.

Table 1: Site AZ1 calculated thermal conductivity for 0.2 m depth intervals centered on each sensor depth. Calculated cumulative thermal diffusivity between the surface and each sensor depth.

Depth	Thermal conductivity	Thermal resistance
0.10 m	1.15 W/mK	0.089 m^2K/W
0.30 m	1.11 W/mK	0.270 m^2K/W
0.50 m	0.64 W/mK	0.516 m^2K/W
0.70 m	0.66 W/mK	0.824 m^2K/W
0.90 m	0.75 W/mK	1.109 m^2K/W
1.10 m	0.85 W/mK	1.360 m^2K/W

2.1.3 AZ1 mean daily conductive heat flow

As described by Equation 3, conductive heat flow is the gradient of temperature versus thermal resistance, visually represented by a 'Bullard plot.' A Bullard plot deviates from linear if there is a transient component to heat flow, as is almost always the case in the top meter of the ground. A straight line of best fit through a Bullard plot, however, approximates the mean conductive heat flow over the sampled depth interval at the time of the temperature measurements. Figure 9, for example, shows the Bullard plots and conductive heat flows calculated from the 24-hour mean temperatures on seven different days during the Heat Needle trial at site AZ1.

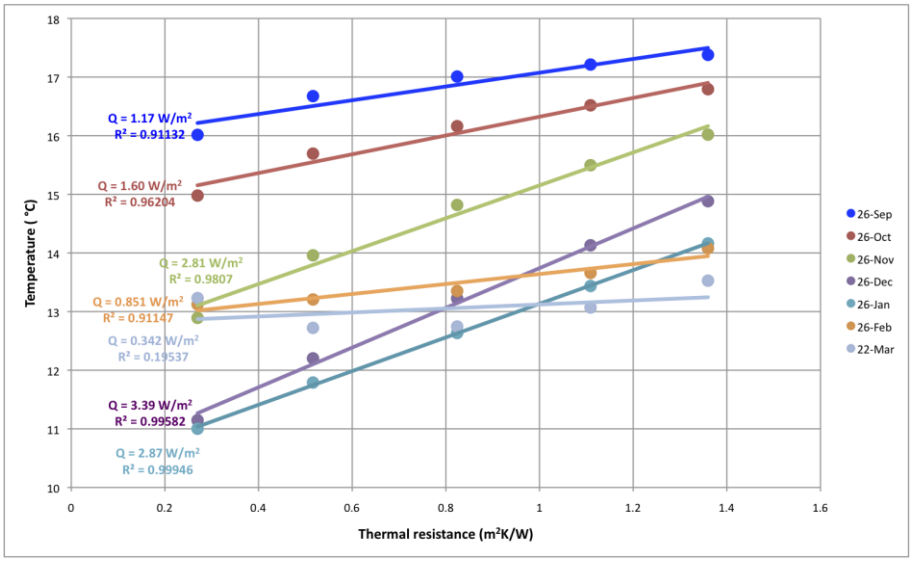

Figure 9: 24-hour mean temperature versus thermal resistance ('Bullard plot') for selected days at site AZ1. The gradients (designated by "Q") approximate the mean conductive heat flows for the given days over the sampled depth interval.

The bold line on Figure 10 presents the daily mean conductive surface heat flow as a function of time over the trial period at site AZ1, based on the temperature records on Figure 7. The rise in heat flow over the first three months of the record is a response to the seasonal decrease in surface temperature over that period. A seasonal correction can be approximated from the observed decrease in mean surface temperature between the equinox and the solstice (~6.5°C), the thermal diffusivity of the ground estimated from the phase lag of the daily temperature signal to 1.10 m (2.5 x 10^{-7} m^2/s), and an assumed 365.25-day periodic surface temperature cycle. The thin line on Figure 10 shows the corrected heat flow, which retains the noise of surface temperature fluctuations due to weather systems.

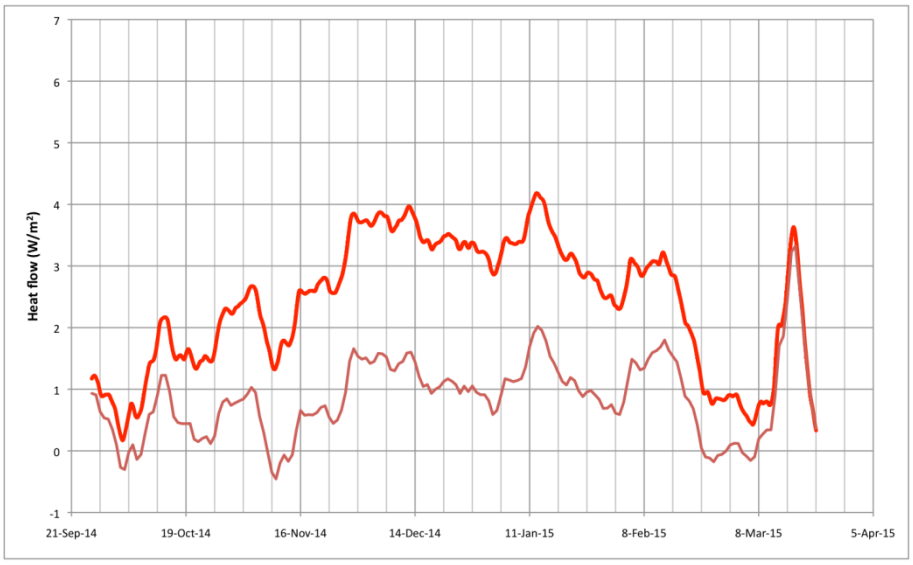

Figure 10: Daily mean conductive surface heat flow versus time for site AZ1 (bold line); approximately corrected for seasonal surface temperature trend (thin line). Horizontal grid interval is one week.

2.2 Temperature records and thermal conductivity tests at sites AZ2, AZ4, AZ6, AZ7 and AZ8

Collection and processing of Heat Needle data at the other five sites (Table 2) followed the same procedures as described for site AZ1 above. A full temperature record was collected at all sites except AZ7, where many data were recorded as 'null' or corrupted due to a logger installation error. Thermal conductivity and thermal diffusivity profiles were successfully calculated for all sites, with results summarized in Table 3, but the missing temperature data resulted in gaps in the daily mean heat flow calculated for site AZ7.

Table 2: Locations of sites AZ2, AZ4, AZ6, AZ7 and AZ8.

Site	Site name and description	Latitude Longitude	UTM Zone 14Q Coordinates Elevation	Google Earth image (± 5 m)
AZ2	**Balneario Rancho Viejo** Inside the grounds of a private spa, fenced with permanent surveillance. Heat Needle installed about 3 m from a 1 m deep and 3 m wide flowing creek.	19.78203 °N 100.67619 °W	2188230 mN 324402 mE 2,776 ± 9 m	

AZ4	**Balneario La Cumbre** Inside the boundary of a small private spa. The lot was completely fenced and under permanent surveillance.	19.82160 °N 100.68566 °W	2192620 mN 323454 mE 2,799 ± 13 m	
AZ6	**Drilling pad for well AZ-41** On CFE property at the edge of the pad of geothermal well AZ-41. Fenced but not under constant surveillance.	19.81407 °N 100.67686 °W	2191778 mN 324367 mE 3,050 ± 11 m	
AZ7	**Drilling pad for well AZ-26** On CFE property on the pad of geothermal well AZ-26. Fenced and secure.	19.78202 °N 100.65013 °W	2188202 mN 327133 mE 2,937 ± 7 m	
AZ8	**Poblado La Yerbabuena** Adjacent to a CFE seismic station on the outskirts of the village of La Yerbabuena. The location, outside the geothermal field, was isolated but not fenced.	19.80659 °N 100.71952 °W	2190995 mN 319890 mE 2,558 ± 12 m	

Table 3: Top numbers: Mean thermal conductivities (W/mK) for 0.2 m depth intervals centered on each sensor depth. Bottom numbers: Mean thermal diffusivity (m^2K/W) between the surface and each sensor depth.

Depth	AZ2	AZ4	AZ6	AZ7	AZ8
0.10 m	0.61 0.163	0.80 0.125	0.92 0.109	1.10 0.091	0.60 0.166
0.30 m	0.69 0.471	0.85 0.368	1.31 0.294	1.03 0.280	0.88 0.446
0.50 m	0.70 0.759	1.06 0.580	0.92 0.479	1.25 0.458	0.74 0.695
0.70 m	0.84 1.022	0.94 0.781	0.78 0.716	1.19 0.622	0.74 0.965
0.90 m	0.88 1.256	0.98 0.990	0.68 0.992	1.00 0.807	0.75 1.234
1.10 m	1.50 1.436	1.00 1.192	0.65 1.293	1.10 0.998	0.75 1.501

2.3 Results of heat flow calculations

Figure 11 shows the daily mean surface temperatures recorded at all six sites presented on the same axes. While the sites were clearly correlated on the scale of weeks to months, variation in mean surface temperature was as much as 5°C on any given day. If the surface temperatures were identical at all sites, then differences in calculated conductive heat flow would be due entirely to subsurface effects (geothermal heat and thermal diffusivity). But variations in surface temperature complicated the processing and interpretation of the results. Specifically, the different sites required different magnitudes of correction for the annual surface temperature cycle.

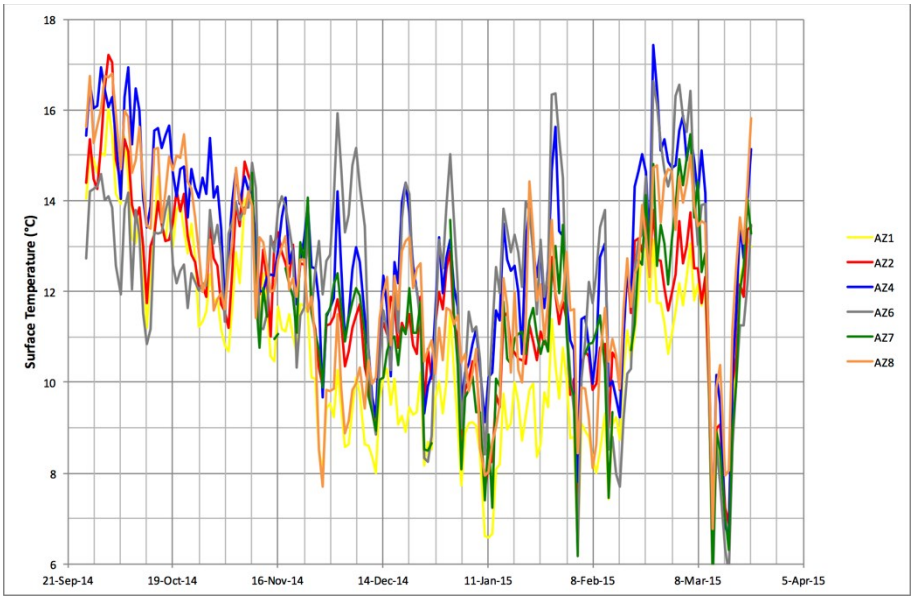

Figure 11: Daily mean recorded temperature of the ground surface at all six trial sites. Horizontal grid interval is one week.

Figure 12 shows the calculated conductive surface heat flow through time at the six sites on the same set of axes. The relative differences in heat flow between sites are not immediately apparent for much of the record. They are clearer, however, on Figure 13, which shows the same surface heat flow series after corrections for assumed sinusoidal annual surface temperature cycles. Differences between sites are clearer still on Figure 14, where the corrected heat flow series for sites AZ1, AZ2, AZ4, AZ6 and AZ7 are plotted relative to the 'background' site AZ8.

Figure 14 reveals that the heat flow over the six-month trial was consistently elevated at sites AZ1, AZ2, AZ4 and AZ6 relative to site AZ8. The mean heat flows at sites AZ1, AZ2 and AZ4 were indistinguishable from each other within the 'weather system' noise (± 0.5 W/m^2), with all three sites about 1.0 W/m^2 higher than at AZ8. Heat flow at site AZ6 was notably higher, at about 2.5 ± 0.5 W/m^2 above AZ8. The surface heat flow calculated at site AZ7 was not significantly greater than the 'background' site AZ8. This is surprising given that AZ7 is located within the geothermal field and might be expected to have greater than regional background heat flow. This could be due to the following causes:

- Geothermal heat flow at site AZ7 might be the same as the regional background. This would be surprising given that the site coincides with a production well intersecting a high temperature geothermal reservoir at depth.
- Shallow advective groundwater flow or rain infiltration might have effectively 'flushed' the geothermal heat before it reached the surface. This is always possible in areas of high topographic relief and/or permeable ground. AZ7 was on the edge of an alluvial valley, the top few meters of which could be highly permeable.
- Man-made disturbances to the surface conditions in the recent past might have increased the mean surface temperature. An increase in the amount of surface solar heating can have the transient effect of reducing near-surface thermal gradient, and hence heat flow, until thermal re-equilibration is reached. This is possible at AZ7, given the land clearing around the site.

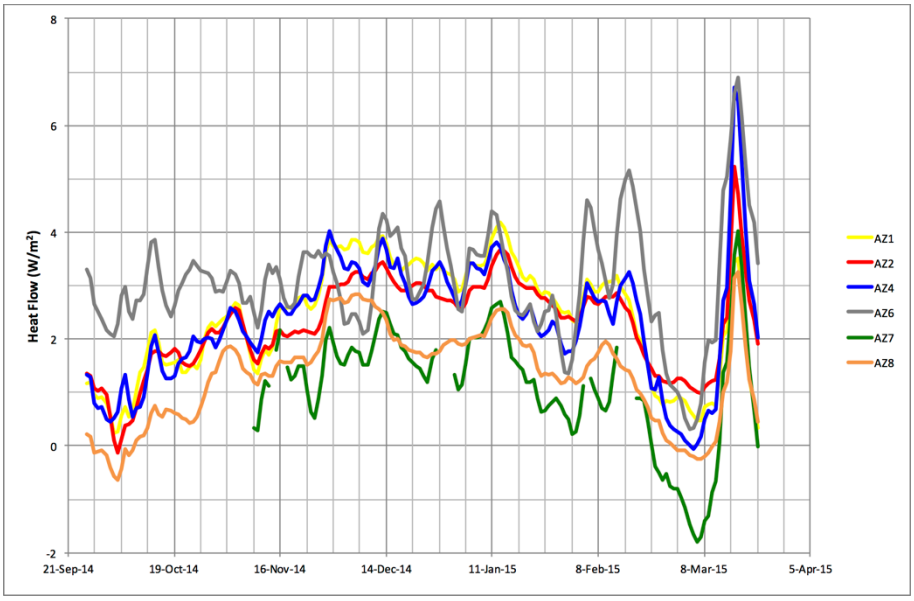

Figure 12: Daily mean conductive surface heat flow (W/m^2) versus time for all six sites. Horizontal grid interval is one week.

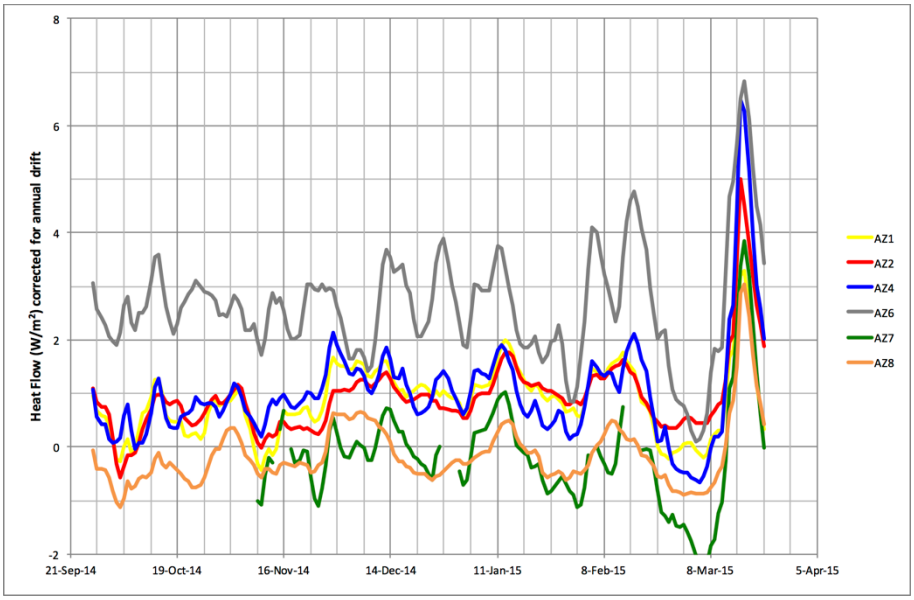

Figure 13: Daily mean conductive surface heat flow (W/m^2) corrected for the seasonal surface temperature cycle. Horizontal grid interval is one week.

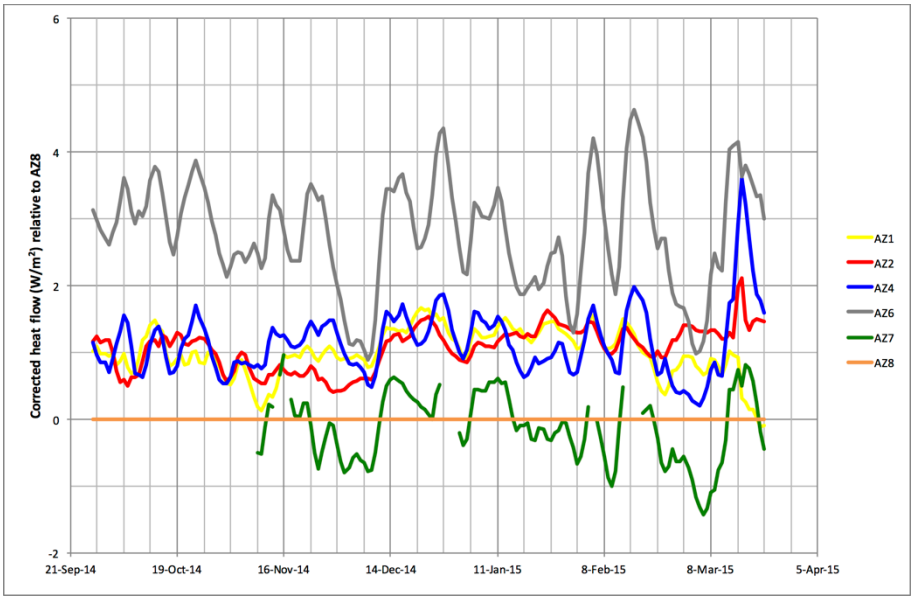

Figure 14: Daily mean conductive surface heat flow (W/m^2) corrected for the seasonal surface temperature cycle, relative to 'background' site AZ. Horizontal grid interval is one week.

3. SUMMARY OF FINDINGS AND CONCLUDING REMARKS

3.1 Performance of Heat Needles

The trial of six Heat Needles was successfully completed in the Los Azufres geothermal area over a six-month period from September 2014 to March 2015. The Heat Needles were relatively simple to deploy and retrieve. No casings suffered any damage during deployment and all were subsequently recovered in re-usable condition. Passive temperature measurements were simple and effective over the six-month measurement period, recording accurate and precise variations in shallow thermal gradient through time except at site AZ7, where a significant portion of data was corrupted due to a logger installation error.

Thermal conductivity measurements were carried out successfully at all sites. When the results of these were combined with the temperature records, the Heat Needles revealed lateral variations in geothermal heat flow to a precision of ± 0.5 W/m^2 between the six survey sites. Heat flow at site AZ6 was the highest at 2.5–3.0 W/m^2 above background; heat flow at sites AZ1, AZ2 and AZ4 were each about 1.0 W/m^2 above background; and heat flow at site AZ7 was indistinguishable from background.

3.2 Comparison with other thermal survey types

The Heat Needle results can be compared to those that a 'ground temperature survey' might have produced. Figure 15 shows the recorded temperatures at 1.10 m depth at the five 'in field' sites relative to the ground temperature at the 'background' site AZ8 over the six-month period. The conclusions from single-depth ground temperature measurements alone would be different to the heat flow results. While ground temperature alone would have identified that site AZ6 was significantly hotter than site AZ8 at any time over the six month period, the magnitude of the apparent anomaly would depend on the time at which the measurements were made. Furthermore, for most of the six-month period, a ground temperature survey would have failed to detect a significant thermal anomaly at site AZ1 and would have identified a *negative* anomaly at site AZ7. Site AZ4 would have appeared hotter than site AZ2 at all times.

The Heat Needle results can also be compared to estimates of conductive heat flow based on the observed thermal gradient in stabilized zones of deep geothermal wells drilled by CFE in the Los Azufres geothermal field. Table 4 presents the results for four wells, the locations of which can be seen on Figure 2. The values are taken from previous work (Garcia Estrada *et al*. 2001), and from the work of O.M. Espinoza-Ojeda (this paper). Thermal conductivity was not measured, but assumed from typical values reported in literature for the types of rocks intersected by the wells. Relative to the Heat Needle locations, well AZ-22 is about 500 m from site AZ1, well AZ-26 is adjacent to site AZ7, well AZ-37 is less than 1 km from site AZ2, and well AZ-41 is adjacent to site AZ6.

The two heat flow values estimated for well AZ-22 differ because different gradient intervals were used in each case, but both are broadly consistent with the Heat Needle result for site AZ1. The two heat flow estimates for well AZ-26 also differ because of different gradient intervals. The value published by Garcia Estrada *et al*. (2001) (0.26 W/m^2) is consistent with the result for site AZ7 (0.0 ± 0.5 W/m^2), although the significance of the Heat Needle surface heat flow result with respect to deeper heat flow at site AZ7 was discussed in Section 2.3 above. The Heat Needle results for sites AZ2 and AZ6 are both higher than the deep heat flow estimates from the nearest wells (AZ-37 and AZ-41, respectively), significantly so at site AZ6. Given their proximity to surface thermal manifestations (see Figure 2), the surface heat flow at both Heat Needle sites might be influenced by hot water rising through relatively shallow fractures.

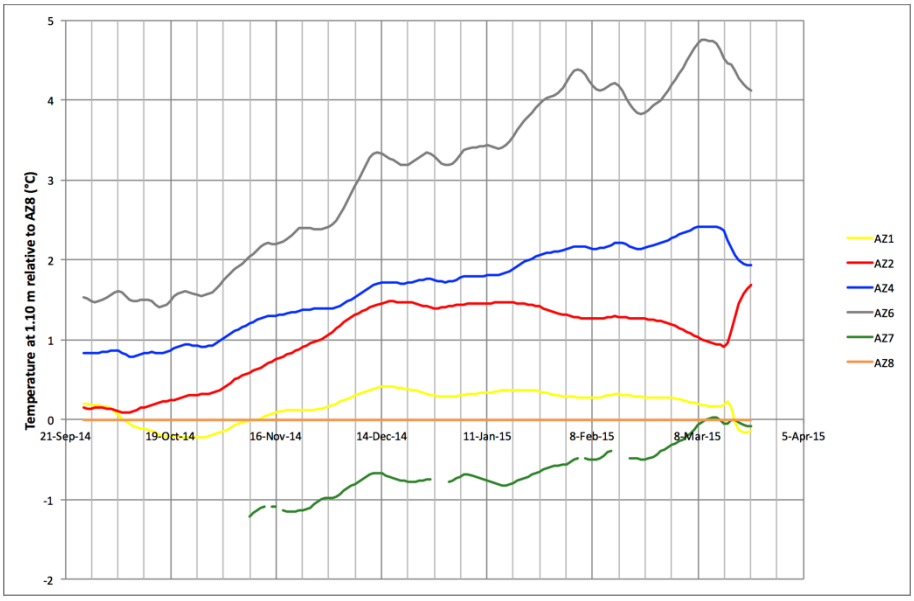

Figure 15: Daily mean recorded temperature at 1.10 m depth relative to site AZ8. Horizontal grid scale is one week.

Table 4: Heat flow estimated for conductive intervals of several wells in the Los Azufres geothermal field from stabilized thermal gradients and assumed thermal conductivity values. "OEO" = Orlando Espinosa-Ojeda.

Well	Gradient (°C/m)	Conductivity (W/mK)	Heat flow (W/m^2)	Source	Nearest Heat Needle result (W/m^2 above background)
AZ-22	0.45	2.3	1.0	OEO	1.0 ± 0.5 (AZ1)
AZ-22	0.22	2.2	0.48	Garcia Estrada *et al*. (2001)	1.0 ± 0.5 (AZ1)
AZ-26	0.33	2.4	0.79	OEO	0.0 ± 0.5 (AZ7)
AZ-26	0.12	2.2	0.26	Garcia Estrada *et al*. (2001)	0.0 ± 0.5 (AZ7)
AZ-37	0.10	2.3	0.23	OEO	1.0 ± 0.5 (AZ2)
AZ-41	0.08	2.3	0.18	OEO	2.5 ± 0.5 (AZ6)

3.3 Site selection

Our calculation of corrected surface heat flow implicitly assumed that the annual surface temperature cycle had remained relatively stable at each site for a long period. This assumption could be invalid if the land use had recently been changed. Land clearing, for example, can result in a sudden increase in mean surface temperature as more direct sunlight reaches the ground, resulting in a transient reduction in near-surface thermal gradient and heat flow. A 'rule of thumb' for site selection could be that the land surface should not have significantly changed for at least one year for each meter radius of area around the measurement site.

Sites should furthermore be selected away from highly permeable ground (where rainfall can percolate quickly into the ground and alter the near surface geotherm) and suspected aquifer recharge zones (which can 'flush' heat away before it reaches the surface). The sites in this trial were selected largely for ease of access, security and proximity to surface manifestations, and were probably all compromised to some extent with respect to accurately discriminating geothermal heat flow from transient near-surface effects. The thermal states of all six sites were likely disturbed to a greater or lesser extent by land clearing and/or shallow groundwater movements.

Heat Needles measure conductive heat flow at the earth's surface. They are best suited to delineating shallow thermal features such as outflow pathways or permeable fractures, constraining the total heat flux from a geothermal system, or constraining the lateral extent of deep thermal anomalies with carefully designed surveys. Closely spaced sites selected for minimum transient surface disturbances could minimize the thermal disturbance of land clearing and resolve shallow groundwater flow paths.

3.4 A comment on the precision of current interpretations

Heat Needles are designed to measure heat flow to a precision on the order of ± 0.01 W/m^2. That is, they are capable of discriminating heat flow differences between sites to a considerably greater precision than the ± 0.5 W/m^2 achieved in this trial. The current limiting factor on precision is the sophistication of the processing algorithms. The rudimentary algorithms applied in this trial only provided for coarse interpretations. It is encouraging that even those coarse interpretations revealed heat flow variations between the trial sites.

HDR is developing more sophisticated data processing algorithms. For example, the seasonal corrections applied in this trial were based on estimates of thermal diffusivity derived from visual estimation of the time lag of the daily surface temperature cycle as it was detected by progressively deeper sensors. This manual process was prone to subjective judgments as the signals were heavily attenuated at the deeper sensor levels. Uncertainties in the interpreted thermal diffusivity translate into uncertainties in the seasonal correction. Objective methods of calculating thermal diffusivity will greatly improve the accuracy of seasonal corrections.

Furthermore, the corrections reported in this paper only considered the annual temperature cycle. More sophisticated corrections will account for *all* signal frequencies, especially the 'weather system' cycles that tend to have periods on the order of 2–4 weeks. Correcting for these shorter-period cycles should resolve heat flow variations between sites to a much greater resolution than ± 0.5 W/m^2. These and other advances in data processing should lead to progressively greater precision in the interpretation of surface heat flow relative to 'background' sites.

ACKNOWLEDGEMENTS

The authors wish to thank the Fondo de Sustentabilidad Energética SENER-Conacyt for providing the funds to develop this work, through the CeMIE-Geo's Project 23: Testing probes for measuring shallow heat flow in geothermal zones. We also thank the geothermal division of the CFE for their support and collaboration in Los Azufres geothermal field.

REFERENCES

Arellano-G., V.M., Ramírez-M., M., Barragán-R., R.M., Paredes-S., A., Aragón-A., A., López-B., S. and Casimiro-E., E.: Condiciones termodinámicas de los fluidos del yacimiento de Los Azufres (México) y su evolución en respuesta a la explotación (1979-2011). *Memorias del XXII Congreso Anual de la Asociación Geotérmica Mexicana*, Cuernavaca, Mor., Mexico, 10-11 de Marzo (2015).

Barragán Reyes, R.M., Arellano Gómez, V.M., Mendoza, A. and Reyes, L.: Variación de la composición del vapor en pozos del campo geotérmico de Los Azufres, México, por efecto de la reinyección. *Geotermia*, 25(1), 3–9 (2012).

Beardsmore, G.R.: Towards a shallow heat flow probe for mapping thermal anomalies. *Proceedings,* 37th Workshop on Geothermal Reservoir Engineering, Stanford University, Stanford, CA, January 30 - February 1 (2012).

Beardsmore, G.R. and Antriasian, A.: Developing the 'Heat Needle'—a tool for cost effective heat flow mapping. *Proceedings,* World Geothermal Congress, Melbourne, Australia, 19–25 April (2015).

Blackwell, J.: A transient-flow method for determination of thermal constants of insulating materials in bulk (part 1— theory). *Journal of Applied Physics*, 25, 137–144 (1954).

Carslaw, H.S. and Jaeger, J.C.: *Conduction of Heat in Solids, Second Edition*. Oxford University Press, Oxford UK (1959).

Coolbaugh, M., Sladek, C., Zehner, R., and Kratt, C.: Shallow temperature surveys for geothermal exploration in the Great Basin, USA, and estimation of shallow aquifer heat loss. *GRC Transactions*, 38, 115–122 (2014).

Dobson, P.F. and Mahood, G.A.: Volcanic stratigraphy of the Los Azufres geothermal area, Mexico. *Journal of Volcanology and Geothermal Research*, 25, 273–287 (1985).

García Estrada, G., López Hernández, A. and Prol Ledesma, R.M.: Temperature-depth relationships based on log data from the Los Azufres geothermal field, México. *Geothermics*, 30, 111–132 (2001).

Gutiérrez-Negrín, L.C.A.: Mexican Geothermal Plays. *Proceedings World Geothermal Congress 2015*, Melbourne, Australia, 19–25 April (2015).

Gutiérrez-Negrín, A. and Aumento, F.: The Los Azufres, Michoacán, Mexico, geothermal field. *Journal of Hydrology*, 56, 137–162 (1982).

Harvey, C., Beardsmore, G., Moeck, I. and Rüter, H.: *Geothermal Exploration, Global Strategies and Applications*. IGA Academy Books, Bochum, Germany (2016).

Pérez Esquivias, H., Macías Vázquez, J.L., Garduño Monroy, V.H., Arce Saldaña, J.L., García Tenorio, F., Castro Govea, R., Layer, P., Saucedo Girón, R., Martínez, C., Jiménez Haro, A., Valdés, G., Meriggi, L. and Hernández, R.: Estudio vulcanológico y estructural de la secuencia estratigráfica Mil Cumbres y del campo geotérmico de Los Azufres, Mich., *Geotermia*, 23(2), 51–63 (2010).

Popov, Y., Beardsmore, G., Clauser, C. and Roy, S.: ISRM suggested methods for determining thermal properties of rocks from laboratory tests at atmospheric pressure. Rock Mechanics and Rock Engineering, 49(10), 4179–4207 (2016).

Viggiano-Guerra, J.C. and Gutiérrez-Negrín, L.C.A.: Comparison between two contrasting geothermal fields in Mexico: Los Azufres and Los Humeros. *Proceedings of the World Geothermal Congress 1995, Volume 3*, Florence, Italy, 18-31 May (1995).